AIAA Aviation
22-26 June 2015, Dallas, TX
15th AIAA Aviation Technology, Integration, and Operations Conference

Identifying Phases of Flight in General Aviation Operations

Valentine Goblet[1], Nicoletta Fala[2], and Karen Marais[3]
Purdue University, West Lafayette, IN, 47907

Identifying phases of flight in General Aviation can help in identifying safety events, which are events which may result in the aircraft being in a hazardous state. Unlike commercial operations that have well-defined phases of flight such as taxi, takeoff, climb, cruise, descent, approach, and landing, GA missions have more hard-to-identify phases of flight. For example, pilot training missions can involve multiple "touch-and-go" maneuvers, which makes it difficult to define a distinct cruise phase during the patterns. Here, we present initial work on automatically identifying phases of flight in GA. We demonstrate our approach on 16 different flight samples from a Cirrus SR20 aircraft equipped with a Garmin G1000 avionics system.

Abbreviations

ASIAS	=	Aviation Safety Information Analysis and Sharing
BTS	=	Bureau of Transportation Statistics
FAA	=	Federal Aviation Administration
FDR	=	Flight Data Recorder
FSI	=	Flight Segment Identification
GA	=	General Aviation
GAMA	=	General Aviation Manufacturers Association
GPO	=	Government Publishing Office
ICAO	=	International Civil Aviation Organization
KIAS	=	Knots Indicated AirSpeed
NTSB	=	National Transportation Safety Board
POH	=	Pilot Operating Handbook
R-ASIAS	=	Rotorcraft ASIAS
RPM	=	Revolutions Per Minute

I. Introduction

General Aviation (GA) is defined as all flight operations, excluding military and scheduled airline operations[1]. Almost 97% of the US civil aviation fleet is composed of GA aircraft[2]. In 2013, 209,034 GA aircraft flew 24.4 million flight hours[1]. In the same year, there were 1,222 GA accidents, which accounted for 94% of all US civil aviation accidents[3]. 18.1% of the GA accident were fatal, resulting in 387 fatalities.

In this paper, we present research to improve GA safety carried out as part of the GA-ASIAS project. GA-ASIAS is one of the projects under the Partnership to Enhance GA Safety, Accessibility, and Sustainability (PEGASAS)—an FAA Center of Excellence for GA. The mission of PEGASAS is to enhance GA safety, accessibility, and sustainability by partnering the FAA with a national network of researchers, educators, and industry leaders. Research efforts to further fixed-wing GA safety are discussed in companion papers[4,5].

One of the goals of GA-ASIAS is to identify and study the safety events that occur during flight and on the ground. In related PEGASAS work on rotorcraft safety, safety events are defined as *one or more exceedances that take place concurrently along with parameters during a specified phase of flight and directly relate to a safety of flight condition*; and we use the same definition in this research. For example, low airspeed at large bank angles is a safety event that can result in an aerodynamic stall. By identifying such safety events for different flight phases, we can inform pilots of situations during flight that pose a high risk of accidents.

[1] Graduate Research Assistant, School of Aeronautics and Astronautics, 701 W. Stadium Ave, Student Member.
[2] Graduate Research Assistant, School of Aeronautics and Astronautics, 701 W. Stadium Ave, Student Member.
[3] Assistant Professor, School of Aeronautics and Astronautics, 701 W. Stadium Ave., Senior Member.

Unlike commercial operations that have well-defined phases of flight such as taxi, takeoff, climb, cruise, descent, approach, and landing, GA missions have more hard-to-identify phases of flight. For example, pilot training missions can involve multiple "touch-and-go" maneuvers, which makes it difficult to define a distinct *cruise* phase during the patterns.

Extensive research has been conducted on identifying phases of flight in commercial operations. Chati and Balakrishnan used Flight Data Recorder (FDR) data to study the performance of Airbus 330-223 engines in all phases of flight[6]. They identified seven phases of flight by using parameters such as latitude, longitude, pressure altitude, ground speed, and their slopes to identify transition points between phases. SVETLANA [Safety (and maintenance) improvement through automated Flight data ANAlysis]—a consortium of European Union nations and Russia defined new flight phases, using the pre-existing ICAO definitions, and developed a robust algorithm for phase of flight identification in commercial aviation[7].

Paglione and Oaks developed two algorithms to identify the different phases of flight using tracked radar surveillance data[8]. Their algorithm determined the horizontal phase of flight (whether the aircraft was flying straight, or executing a turn) and vertical phase of flight (whether the aircraft was ascending or descending). When compared to the legacy algorithm[9] to detect flight phases, this dual approach resulted in lower missed detection rates, with a modest increase in false detection rates. Gong and McNally presented a methodology for the automated statistical analysis of trajectory prediction accuracy as a function of phase of flight (level-flight, climb, descent)[10]. They based their estimates on statistical analyses of 2774 large commercial jet flights, and they showed that prediction anomalies could be detected from the error distributions.

There has been relatively little work in automatic identification of phase of flight in GA. Nguyen and Ward developed and implemented an Artificial Neural Network Situation Recognizer (ANNSR) to identify six flight modes including takeoff, climb, and cruise modes[11]. They compared their approach to a fuzzy logic-based algorithm, and found that the ANN-based algorithm performed better. Kelly and Painter used fuzzy sets in Flight Segment Identification (FSI)[12]. They argued that fuzzy sets enabled them to: (1) overcome the ambiguity of overlapping flight segments (phases), and make a crisp definition of the flight segments; and (2) to estimate the certainty and derive confidences in their FSI algorithm. However, this method is complex and time-consuming.

Here, we present two methods to identify phases of flight in GA operations. We use a sample of 16 flight data samples to develop our methods. Section II defines the different phases of flight and the associated characteristics. We present our approach to identifying different phases of flight in Section III. We discuss the results from the different methods and measure their performance in Section IV. In the last section, we present concluding remarks and direction for future work.

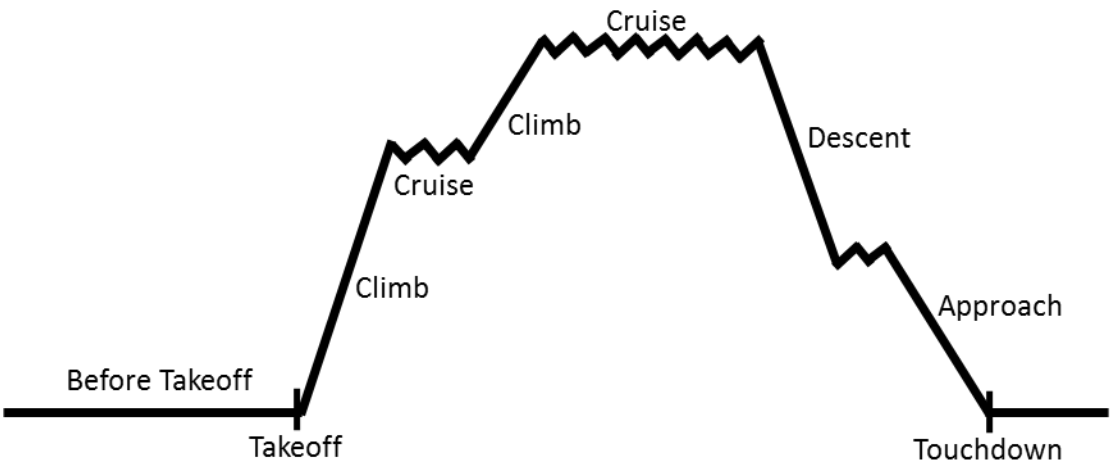

Figure 1: Sample mission profile with phases of flight.

II. Phases of Flight and Safety Events in General Aviation

As mentioned in the introduction, GA phases of flight involve more variation than commercial aviation, which makes it harder to define and identify phases, as highlighted in Figure 1. A higher deviation from the intended flight altitude is expected, compared to commercial flights, for several reasons. First, the mission profiles and purposes of GA flights are more complicated and varied compared to commercial aviation. For example, missions involving crop dusting will have more altitude changes when compared to a commercial aircraft. Second, while commercial pilots

are all required to undergo extensive training, a GA pilot may have as few as 40 hours of flight time including at least 10 hours of solo flight training[13]. Inexperienced pilots may, for example, have trouble maintaining a level cruise altitude. Finally, GA aircraft are usually flown manually, which may result in more variation in altitude, airspeed, and flight path.

Table 1: Safety events specific to phases of flight

Phase of Flight	Safety events
Before takeoff	- Excessive power on the ground - Excessive starter on engagement - Taxi speed on ramp - Taxi speed on taxiways - Hard braking during taxi - Lateral G loads during taxi - Excessive RPM drop during engine run-up
Takeoff	- Heading variation at power application - Low RPM at rotation - Airspeed at liftoff - Angle of attack` - Pitch attitude at takeoff - Flap position at takeoff - Bank angle - Lateral G loads - Runway distance remaining at liftoff - Tail wind component
Climb	- Cross wind component at 100ft - Airspeed on climb between 100ft and 500ft - Bank angle below 400ft - Flap retraction - Detection of altitude decrease below 500ft
Cruise	- Maximum altitude - Minimum recovery altitude - Turbulence encounter - Turbulence penetration speed
Approach	- Glide slope deviation - CDI deviation - Vertical speed below 1000 AGL - Airspeed with flaps - Airspeed without flaps - Glide angle - Flap position - Bank angle below 200 AGL - Tailwind component - Crosswind component
Touchdown	- Pitch attitude - Airspeed with flaps - Airspeed without flaps - Detection of hard landing - Lateral G - Centerline tracking - Bounced landing - Excessive braking - Touchdown point - High G turn

Identifying phases of flight is important because many safety event definitions are specific to phases of flight. Table 1 shows examples of safety events that occur during different phases of flight. Section III gives further detail on the parameters and values that can be used to define and automatically identify each phase of flight. As shown in Table 1, specific safety events are relevant during these phases. For example, low RPM at rotation can lead to a stall and an accident during the takeoff phase.

We defined nine phases of flight, as shown in Table 2. These definitions are based on the National Transportation Safety Board published definitions[14]. We added one phase: go-arounds. Go-arounds represent a critical moment when the pilot has to give particular attention to the airspeed and RPM. We replaced the landing phase with "touchdown", to include both actual landings and touch-and-goes, where the pilot lands on the runway but applies full power again.

Table 2: Definition of Phases of Flight

Phase of Flight	Definition	Notes
Standing	Any time before taxi or after arrival while the aircraft is stationary.	NTSB definition[14] extrapolated to any area where the aircraft is stationary (not only on the ramps or parking areas).
Taxi	The aircraft is moving on the ground prior to takeoff and after landing.	NTSB definition.[14]
Takeoff	From the application of takeoff power, through rotation and to an altitude of 35 feet above runway elevation.	NTSB definition.[14]
Climb	Any time the aircraft has a positive rate of climb for an extended period of time.	The NTSB definition[14] only considers an Initial Climb. We extended this definition to any phase where the pilot wants to reach another flight level. Therefore, climb includes en-route climb. This extended definition allows us to detect safety events that are specific to positive and significant rate of climb.
Cruise	The time period following the initial climb during which the aircraft is in level flight.	From the NTSB En-route phase definition[14].
Descent	Any time before approach during which the aircraft has a negative rate of climb for an extended period of time.	Descent is the same as climb but with a negative rate of climb until the altitude is low enough to become an approach phase.
Approach	From the point of pattern entry, or 1000 feet above the runway elevation, to the beginning of the landing flare.	NTSB definition.[14]
Landing (renamed Touchdown)	From the beginning of the landing flare until the aircraft touches down and exits the landing runway, or comes to a stop on the runway, or when power is applied for takeoff, depending upon the intended action after landing.	NTSB definition.[14]
Go-around	A Go-around is a situation where the pilot is about to make a touchdown but decides to apply full power before the landing gear touches the ground.	We added this definition in order to deal with safety events that may also happen during these critical events.

III. Development of Flight Phase Detection Algorithms

In this section we present several methods that aim to identify and classify flight phases. Those methods are based on one or multiple parameter identification. We first give an overview of the data available to us, and then study the methods and their respective results.

A. Test Data

We obtained flight data from 16 flights from Cirrus SR20 aircraft. The length of the flights ranged from 77 minutes for flight training missions to 198 minutes for cross-country flights. All 16 flights in our sample originated from West Lafayette, IN. The aircraft had a Garmin G1000 avionics system on-board, which recorded 66 parameters (e.g., altitude, engine RPM, and pitch angle) at 1 Hz.

B. Easily Identified Flight Phases

While climb, cruise, and descent can be ambiguous in GA, the remaining phases are clearly defined and can be easily identified, as shown in Table 3. We obtained the numerical constraints for the Cirrus SR20 from the Pilot Operating Handbook (POH). Using the parameters and values given in Table 3 for the Cirrus SR20, we were able to correctly identify these phases of flight in all 16 samples. The remainder of this paper focuses on the climb, cruise, and descent phases.

Table 3: Simple Phases of Flight parameters, with values for the Cirrus SR20[15]

Phase of Flight	Identifying Parameters	Notes
Standing	Groundspeed (=0 KIAS) Indicated airspeed (=0 KIAS)	To be certain that the aircraft is stationary on the ramp or parking area, we assume that the aircraft is standing when both groundspeed and indicated airspeed are zero. If we only use groundspeed to identify time periods when the aircraft is standing, we could misidentify cruise portions as standing (e.g. slow flight with a strong headwind). Only looking at airspeed is not sufficient, as airspeed is usually zero until the aircraft is fast enough to take off.
Taxi	Groundspeed (<25 KIAS) Indicated airspeed (=0 KIAS)	Based on the flying behavior we observed in our dataset, we assume that the aircraft is taxiing when its groundspeed is between 0 and 25 KIAS with a zero indicated airspeed.
Takeoff	Engine RPM (>2500 RPM)[15] Altitude (<35 ft above the runway elevation)	We have two types of takeoff: those that occur after taxi, and touch-and-goes, where the takeoff occurs right after touchdown. We define application of full power as the increase of engine RPM to over 95% of its maximum value. The aircraft transitions from takeoff to climb at 35 ft above the runway elevation, according to the definition of takeoff in Table 2.
Approach	Altitude (constant decrease <−200 fpm) Altitude (<1000 ft above runway elevation)	Approach is the last part of descent. We therefore add another constraint: approach starts 1000 ft above the runway elevation, as defined in Table 2.
Landing (renamed Touchdown)	Indicated airspeed (<60 KIAS)[15] Altitude (constant decrease <−200 fpm for one minute) = previous Descent considered	During the landing flare and touchdown, we assume that the indicated airspeed is between 25 kts and 60 kts. A series of negative vertical speeds will precede flare and touchdown, and the aircraft will also be descending in approach.
Go-around	Engine RPM (>2500 RPM)[15] Indicated airspeed (>60 KIAS)[15] Altitude (< 400 ft AGL)	During a go-around, the pilot will apply full power to initiate a climb. Since the aircraft will not touch down during a go-around, the altitude has to remain above runway elevation.

C. Method 1: Altitude-Based Identification

It can be difficult to distinguish between climb, cruise, and descent because of the high variability of altitude during cruise phase, especially in GA flights. We began by attempting to identify these phases based on the altitude and climb/descent rate, as shown in Table 4. The constraints are defined in such a way that each point in a flight can be assigned to one and only one phase.

Table 4: Method 1: Altitude-based identification, with values for the Cirrus SR20

Phase of Flight	Identifying Parameters	Notes
Climb	Change in Altitude (constant increase >200 fpm)	Here we choose a gain of altitude of at least 100 feet over 30 seconds, which corresponds to a positive rate of climb of 200 fpm. Choosing 200 fpm identified climbs relatively well. Increasing the value corresponding to the minimum rate of climb will misidentify climb as cruise and decreasing the minimum rate of climb will misidentify cruise segments as climb.
Cruise	Altitude (constant ±200 fpm)	The moving average for a 30 s window of vertical speed should also remain between −200 fpm and +200 fpm. We also have to make sure that cruise flight occurs at an altitude that is above what would be the pattern altitude of the nearest airport.
Descent	Change in Altitude (constant decrease <−200 fpm)	Descent conditions are the reverse of those used to identify a climb. We require a loss of altitude of at least 100 feet over 30 seconds, corresponding to a negative rate of climb of −200 fpm.

Figure 2, Figure 3, and Figure 4 show examples of the method's results for three flights. The "simple" phases are identified as described in Table 3. Note that the touchdown and takeoff phases often follow one another, which means that the pilot did touch-and-goes. The climb, cruise, and descent phases are identified as described in Table 4. The method incorrectly identifies some parts of climbs as cruise (e.g., in Figure 2 at 5414 s seconds, in Figure 3 at 8261 s, and in Figure 4 at 1008 s). Also, some parts of cruise are incorrectly identified as climb (e.g., in Figure 2 at 3742 s, in Figure 3 at 9667 s, and in Figure 4 at 7643 s) or as descent (e.g., in Figure 2 at 2068 s, in Figure 3 at 3938 s, and in Figure 4 at 7525 s). These misidentifications happen because the algorithm is very sensitive to small variations in altitude. We found that attempting to improve identification by adjusting the parameters did not reduce the error rate. Therefore we developed a second method based on smoothing and then assessing the flight data, as described next.

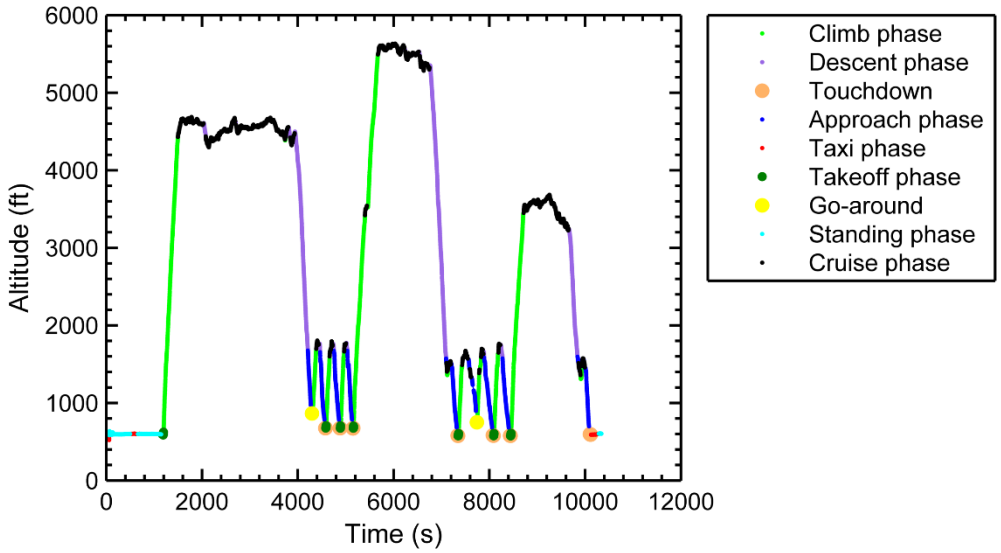

Figure 2: Phases of flight applied to flight sample #12.

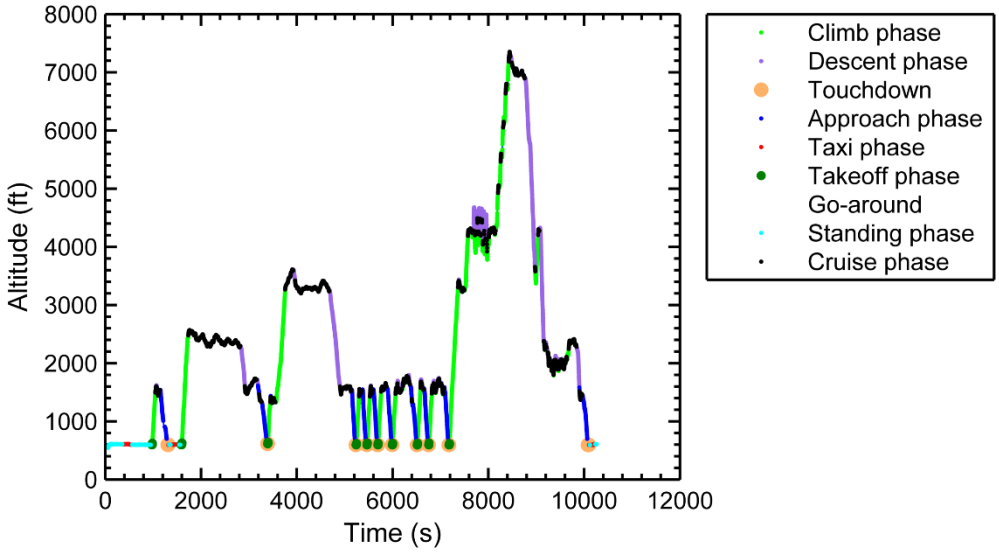

Figure 3: Phases of flight applied to flight sample #9.

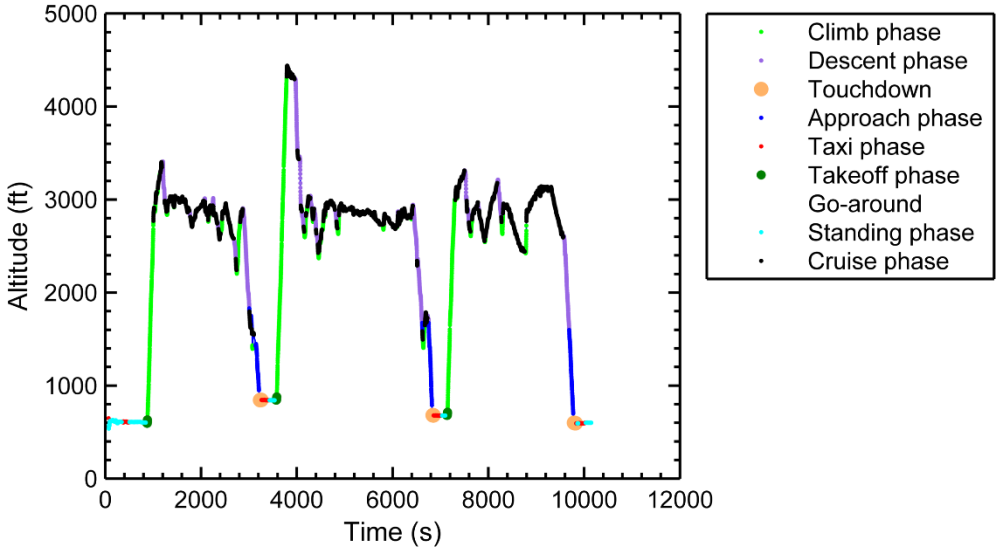

Figure 4: Phases of flight applied to flight sample #1.

D. Method 2: Smoothing and Differentiation Method for Identification

Our second method attempts to address the sensitivity problem by smoothing the data to remove minor short duration variations in altitude. We use three methods to smooth the data, and two methods to subsequently measure the change in altitude. Note that from the point of view of Method 2, approach and takeoff are classified here as descent and climb respectively to simplify the calculations. In practice, these phases will be uniquely identified as discussed in Section III.B.

1. Smoothing Methods

We use three methods to smooth the data. The simplest method is to down-sample the data. Figure 5 shows the result of taking every $n = 100$ points for flight sample #12. The blue line represents the actual altitude as recorded by the FDR and the red line shows the smoothed altitude. As expected, small variations in altitude have been damped, but there is a corresponding loss of information that could lead to misidentification of phases of flight, such as at 5010 s (when the pilot performed a touch-and-go). After this point, the red curve shows a positive slope whereas the actual recorded altitude is still decreasing at the same time. This downside allowed us to try other methods of smoothing the altitude curve. In Section IV we assess the performance of this method for different values of n.

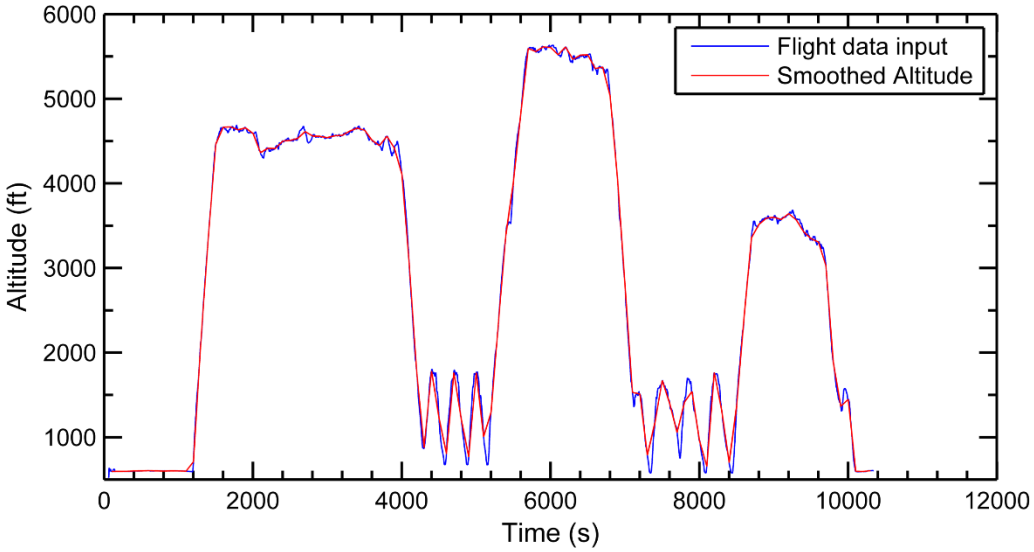

Figure 5: Altitude curve smoothing using the Down-sampling method (n = 100) for flight sample #12.

Our second approach to smoothing is based on the calculation of a moving average over m points, as shown in Figure 6. This approach deals better with go-arounds and touch-and-goes than the down-sampling method, but still misses the peaks and troughs such as at 7725 s. In Section IV we assess the performance of this method for different values of m.

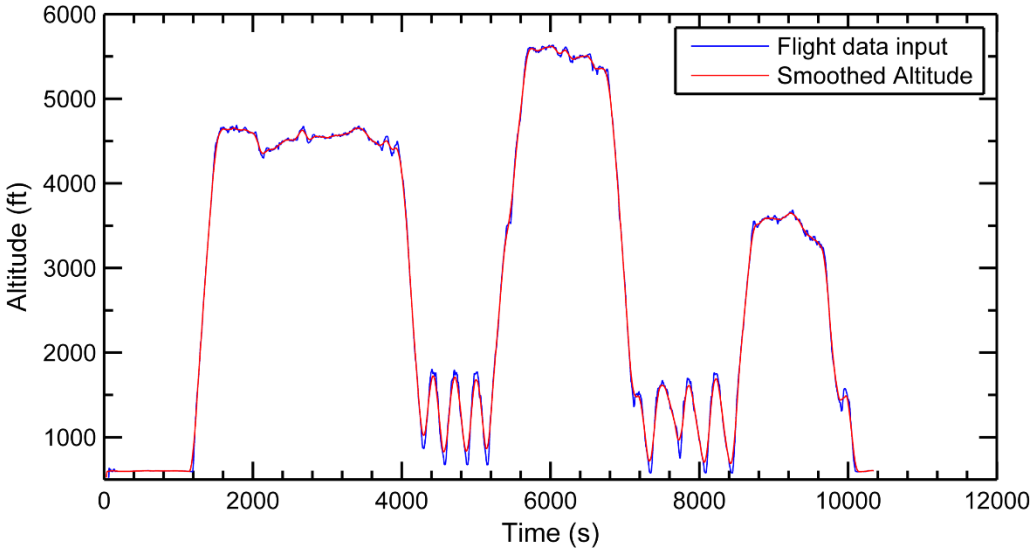

Figure 6: Altitude curve smoothing using the Moving Average method (with m = 100 s span).

Our third approach is based on a local regression method, consisting of a weighted linear least squares and a second degree polynomial model. The local regression method is well-suited to our data because we have no outliers. An example of using local regression is shown on Figure 7. This method deals the best with peaks and troughs, but if the regression is "too good" we return to the problem of spurious identifications. In Section IV we assess the performance of this method for different values of p, the time span over which the local regression is performed.

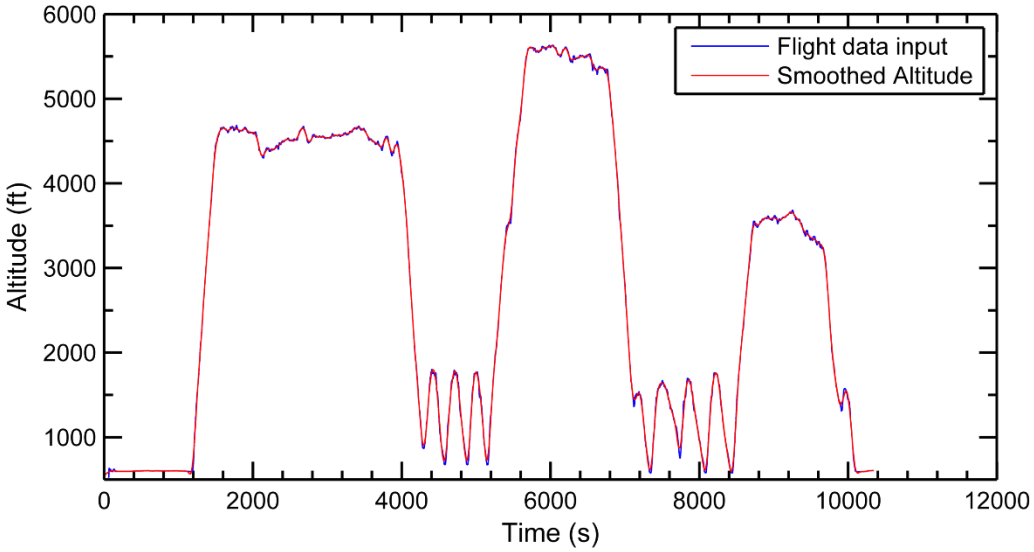

Figure 7: Altitude curve smoothing using the Local Regression method (with p = 200 s span).

2. Differentiation

We use two approaches to assess the change in altitude. Our first approach is based on the change in altitude between adjacent stationary points on the smoothed curve. We identify these points in the code by comparing adjacent points on the smoothed curve and noting when the trend changes from increasing to decreasing, and vice versa.

Figure 8, Figure 9, and Figure 10 show the stationary points as black circles. We define an altitude difference between adjacent stationary points of more than $\Delta h = 1000$ ft as a climb and less than $\Delta h = -1000$ ft as a descent for an altitude greater than 1500 ft AGL (see Table 5). Smaller changes are assumed to be cruise. For altitudes less than 1500 ft AGL, cruise phases are considered only above 500 ft AGL, in order to deal with a constant altitude while the pilot is making a pattern around an airport. The pattern is usually made at 1000 ft above the runway elevation, but we chose to include margins in order to deal with all kinds of trainings and as many situations as possible.

Figure 8, Figure 9, and Figure 10 show the resulting phase identifications for flight sample #12. They show that the results from the differentiation step depend on how the altitude was first smoothed. In particular, down-sampling resulted in a more peaked flight profile than the other two methods. For example, in Figure 8, which shows the results of down-sampling followed by altitude difference, the identified cruise phase beginning at 9101 s is shorter than our manual phase identification (see Figure 18 (a)), which means that cruise-specific safety events may be missed.

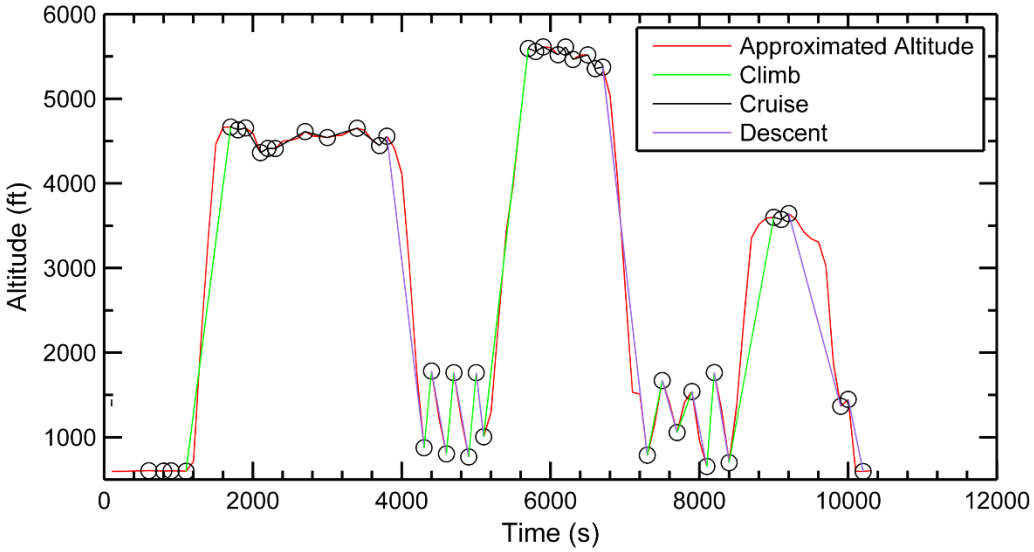

Figure 8: Down-sampling (n = 100), Altitude difference.

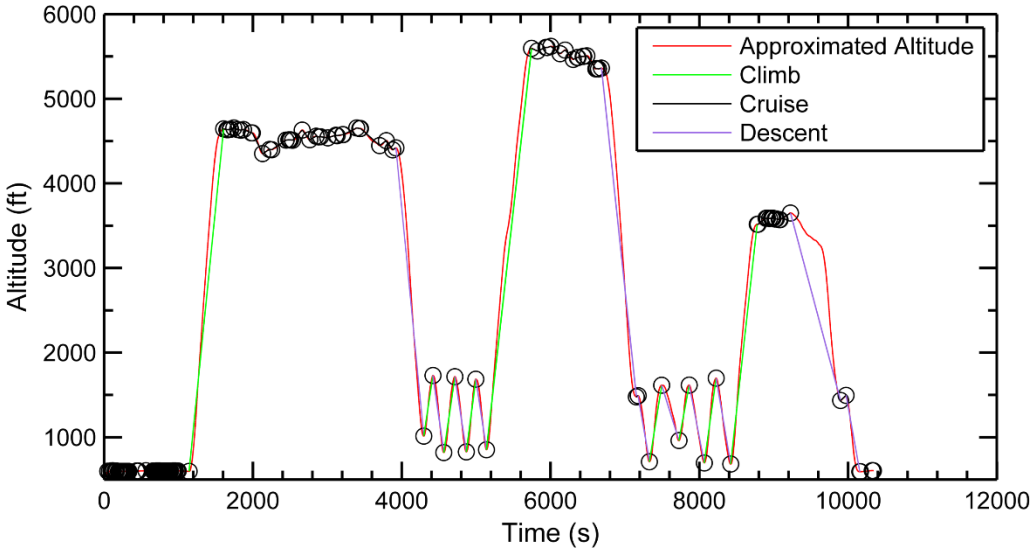

Figure 9: Moving Average (with *m* = 100 s), Altitude difference.

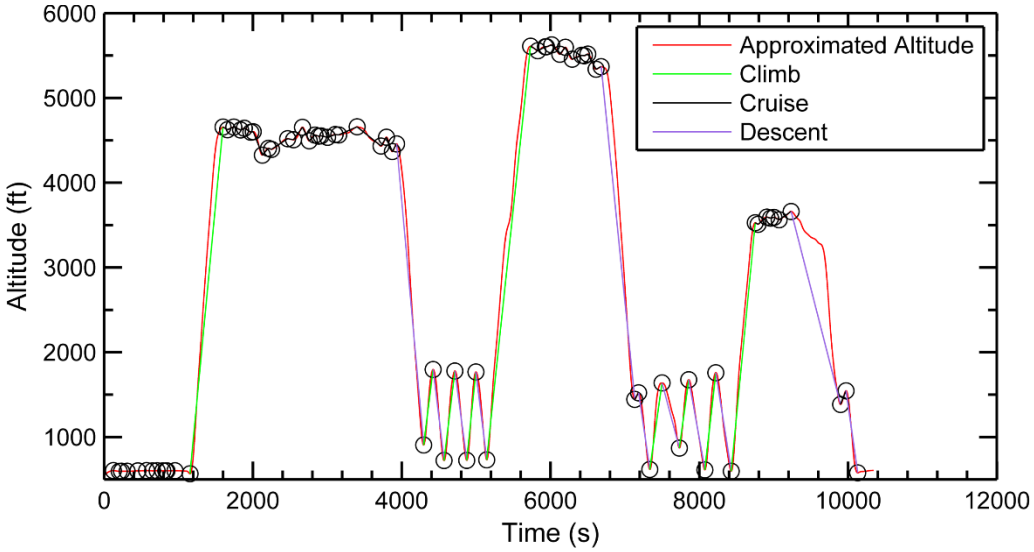

Figure 10: Local Regression (with *p* = 200 s), Altitude difference.

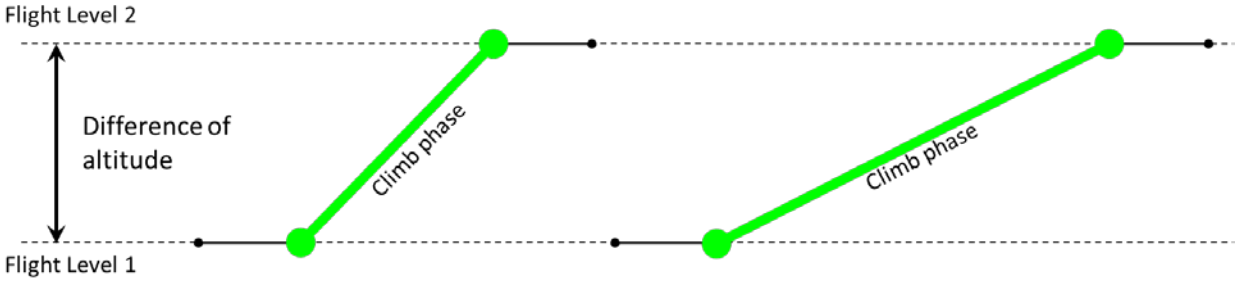

Figure 11: Concept of Altitude Difference.

While this method works fairly well and can detect small changes in altitude, it does not consider the time period over which the climb takes place, as shown in Figure 11. Therefore this method can misidentify slow climbs as climbs and slow descents as descents. From a safety event identification point of view, these slow changes in altitude should

be identified as cruise, since the altitude varies in General Aviation, and a flight with a small slope is closer to a cruise phase in terms of flight parameters.

To address this weakness, our second method is based on the rate of climb over a defined time window. As shown in Table 5, the time window is constant for moving average and local regression methods ($\Delta t = 25$ s), and equal to the down-sampling window n in the down-sampling method. Further, because down-sampling is highly sensitive to n when combining the rate of climb step, we impose an additional constraint that the altitude must be at least 1500 ft AGL, to avoid misidentifying takeoff or landing as climb or descent. The rate of climb/descent requirement is the same as in Method 1.

Table 5: Method 2: Thresholds for the Smoothing and Differentiation Methods

			Down-sampling	**Moving average**	**Local regression**
Altitude Difference	Altitude > 1500 ft AGL	**Climb:**	$\Delta h \geq 1000$ ft	$\Delta h \geq 1000$ ft	$\Delta h \geq 1000$ ft
		Cruise:	-1000 ft $< \Delta h <$ 1000 ft	-1000 ft $< \Delta h <$ 1000 ft	-1000 ft $< \Delta h <$ 1000 ft
		Descent:	$\Delta h \leq -1000$ ft	$\Delta h \leq -1000$ ft	$\Delta h \leq -1000$ ft
	Altitude ≤ 1500 ft AGL	**Climb:**	400 ft $< \Delta h <$ 1000 ft	400 ft $< \Delta h <$ 1000 ft	400 ft $< \Delta h <$ 1000 ft
		Cruise:	-400 ft $< \Delta h <$ 400 ft (only if Altitude > 500 ft AGL)	-400 ft $< \Delta h <$ 400 ft (only if Altitude > 500 ft AGL)	-400 ft $< \Delta h <$ 400 ft (only if Altitude > 500 ft AGL)
		Descent:	-1000 ft $< \Delta h <$ -400 ft	-1000 ft $< \Delta h <$ -400 ft	-1000 ft $< \Delta h <$ -400 ft
Rate of climb	Altitude > 1500 ft AGL	**Climb:**	$\Delta r \geq 200$ fpm	**Climb:** $\Delta r \geq 200$ fpm	**Climb:** $\Delta r \geq 200$ fpm
		Cruise:	-200 fpm $< \Delta r <$ 200 fpm	**Cruise:** -200 fpm $< \Delta r <$ 200 fpm (only if Altitude > 500 ft AGL)	**Cruise:** -200 fpm $< \Delta r <$ 200 fpm (only if Altitude > 500 ft AGL)
		Descent:	$\Delta r \leq -200$ fpm	**Descent:** $\Delta r \leq -200$ fpm	**Descent:** $\Delta r \leq -200$ fpm
	Altitude ≤ 1500 ft AGL	**Climb:**	100 fpm $< \Delta r <$ 200 fpm		
		Cruise:	-100 fpm $< \Delta r <$ 100 fpm (only if Altitude > 500 ft AGL)		
		Descent:	-200 fpm $< \Delta r <$ -100 fpm		
	Minimum time window:		$\Delta t = n$	$\Delta t = 25$ s	$\Delta t = 25$ s

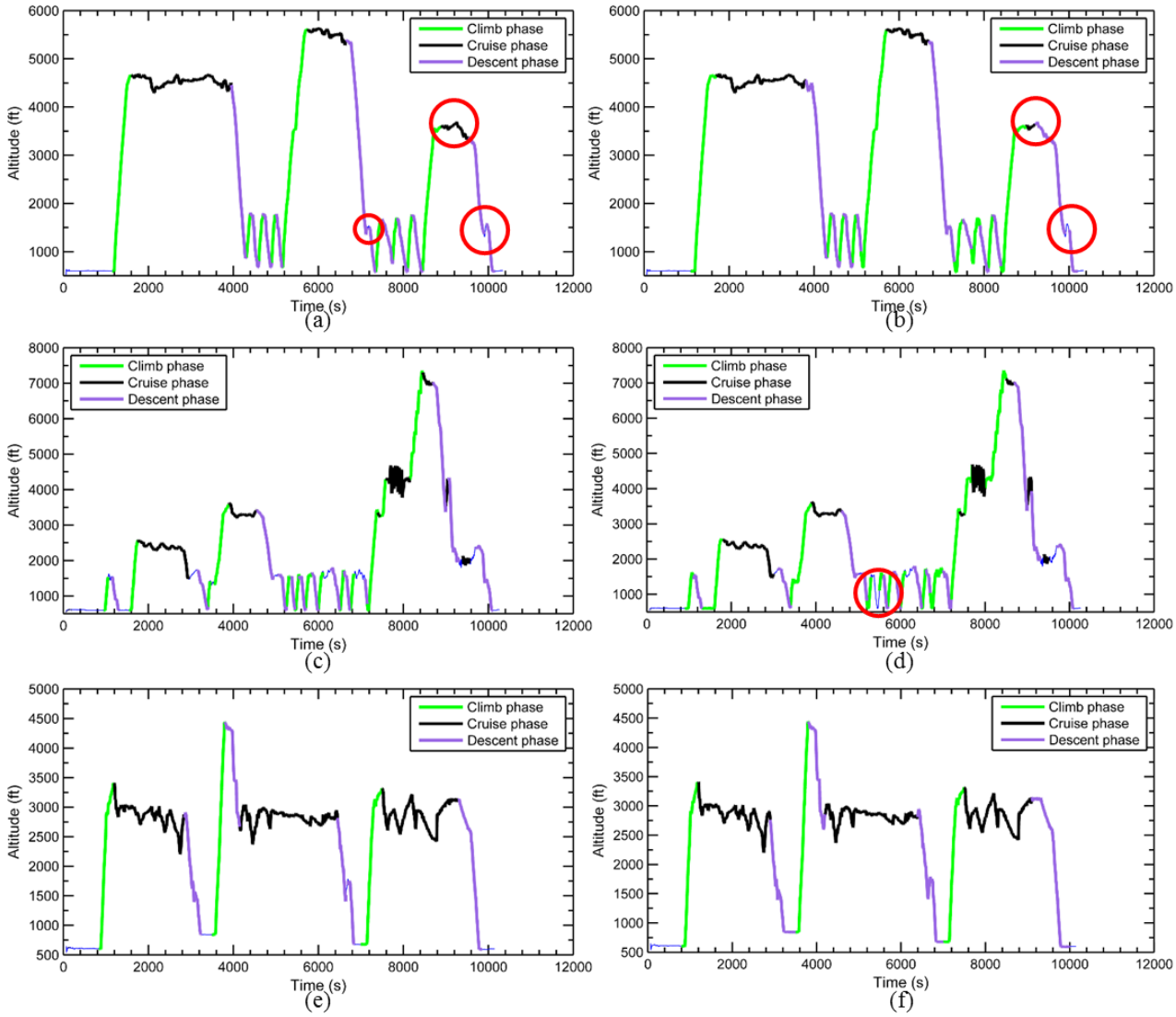

Figure 12: Down-sampling, altitude difference. n = 50 for (a), (c) and (e) and n = 100 for (b), (d), and (f).

Figure 12 shows the results of combining down-sampling and altitude difference for two values of n on three different flights. As indicated by the red circles, some of the climb and descent phases can spill over into the cruise phases. The appropriate value of n also depends on the flight characteristics—for the flight with relatively smooth cruise phases shown in the top row, down-sampling more (n = 100, (b)) works better, but when the flight involves a lot of variation, as in the second row, down-sampling less (n = 50, (c)) works better. Decreasing the value of n increases the accuracy and reduces the amount of spills, but it also increases spurious and incorrect identifications. Therefore the methods must adapt based on the flight characteristics.

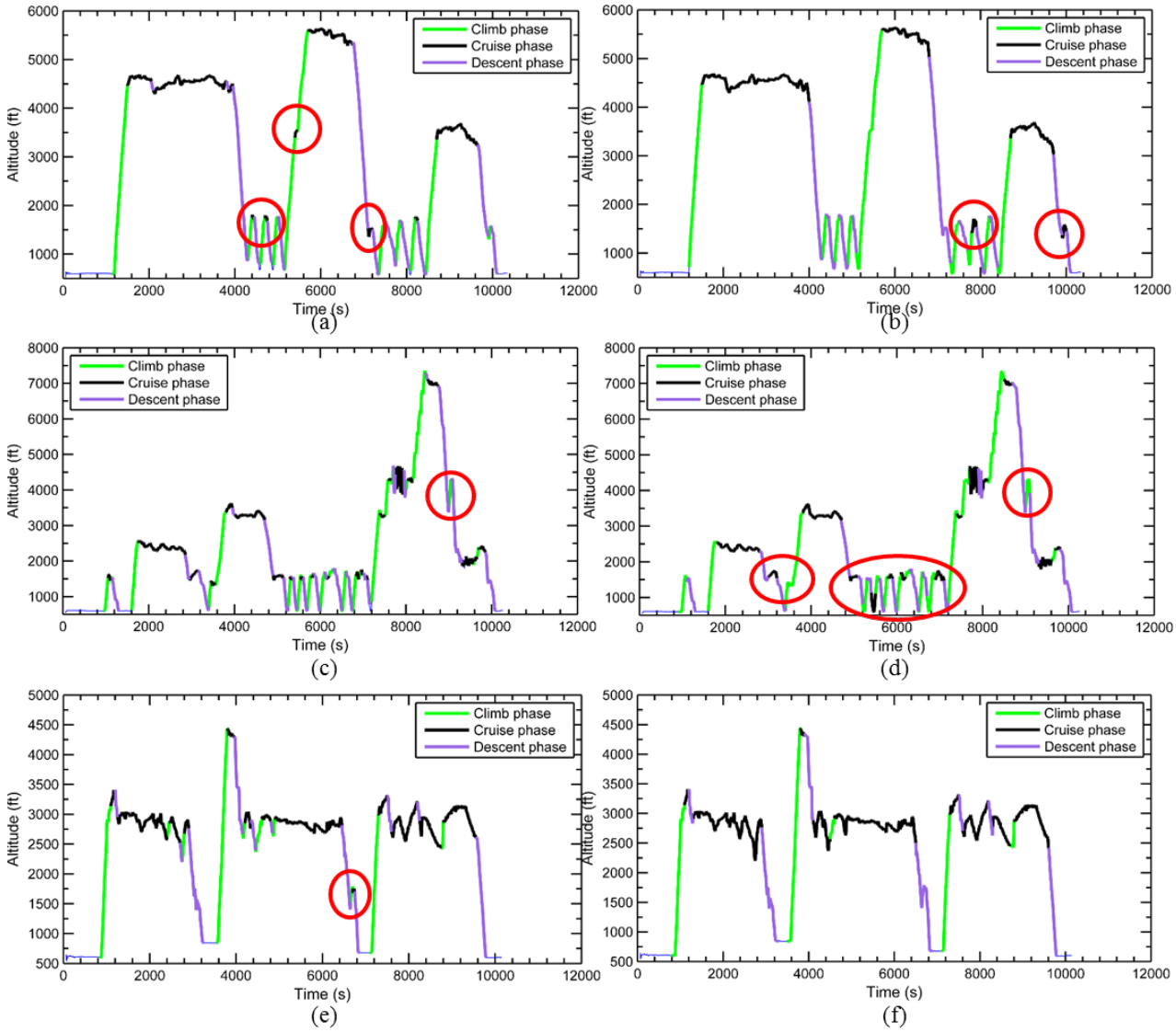

Figure 13: Down-sampling, rate of climb. *n* = 50 for (a), (c), and (e) and *n* = 100 for (b), (d), and (f).

Figure 13 shows the results of combining down-sampling and rate of climb for two values of *n* on three different flights. This combination of methods is better than the previous method at identifying the final cruise segment in the relatively regular flight (top row). However, for the more varied flight (second row), this combination misidentifies some of the touch-and-goes as cruise, and some cruise segments as climb. When *n* increases (right column), it tends to add more misidentifications especially for cases (c) and (d), which both involved a lot of patterns around the airfield.

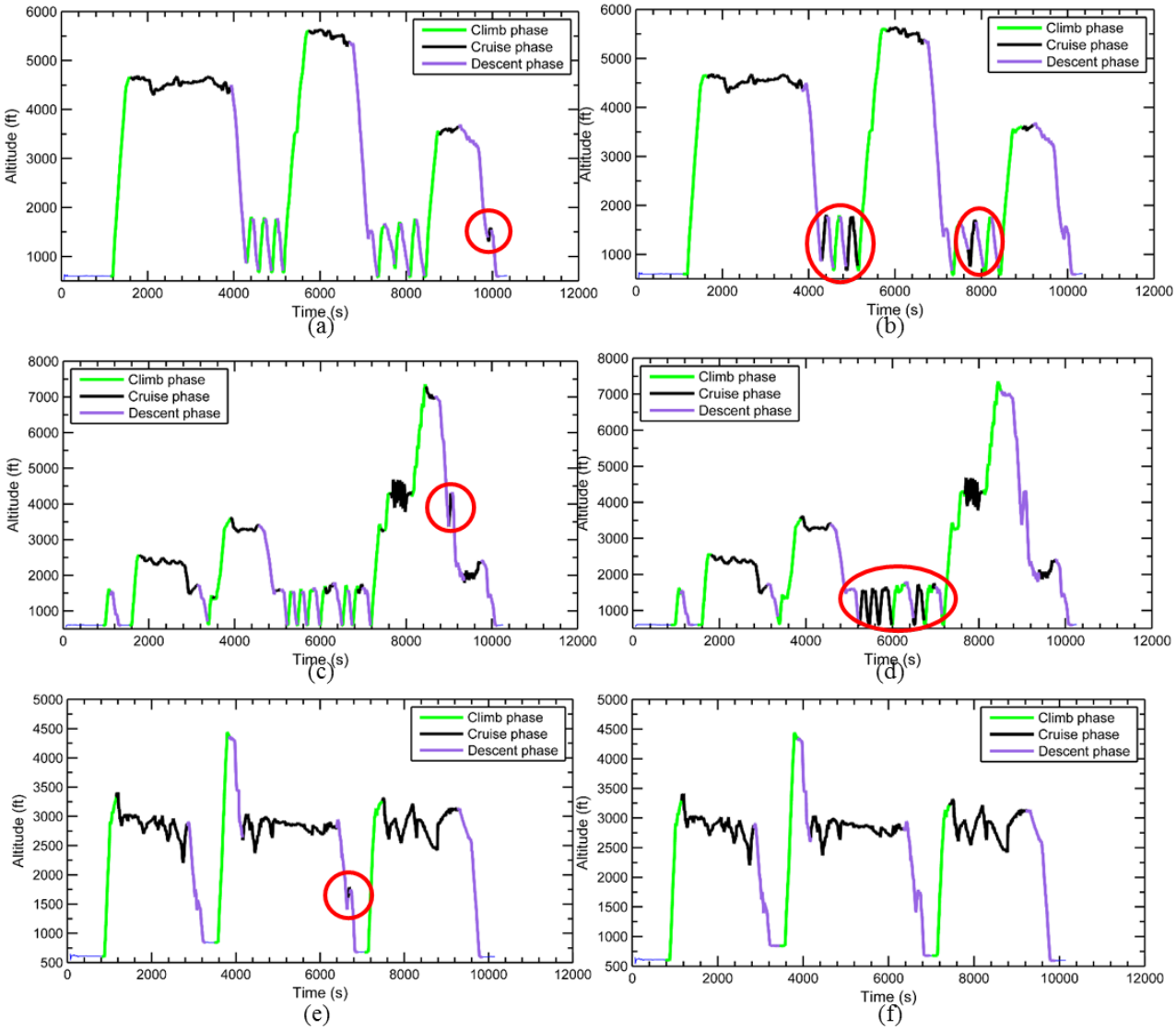

Figure 14: Moving average, altitude difference. *m* = 100 s for (a), (c), and (e), and *m* = 200 s for (b), (d), and (f).

Figure 14 shows the results of combining moving average and altitude difference for two values of *m* on three different flights. The left column shows the results of using a smaller window, and the right column shows the results of using a larger window. The larger window is better when the cruise phase is characterized by a large variation of altitude (last row), and the smaller window is better when the flight sample contains several patterns around the airfield (second row).

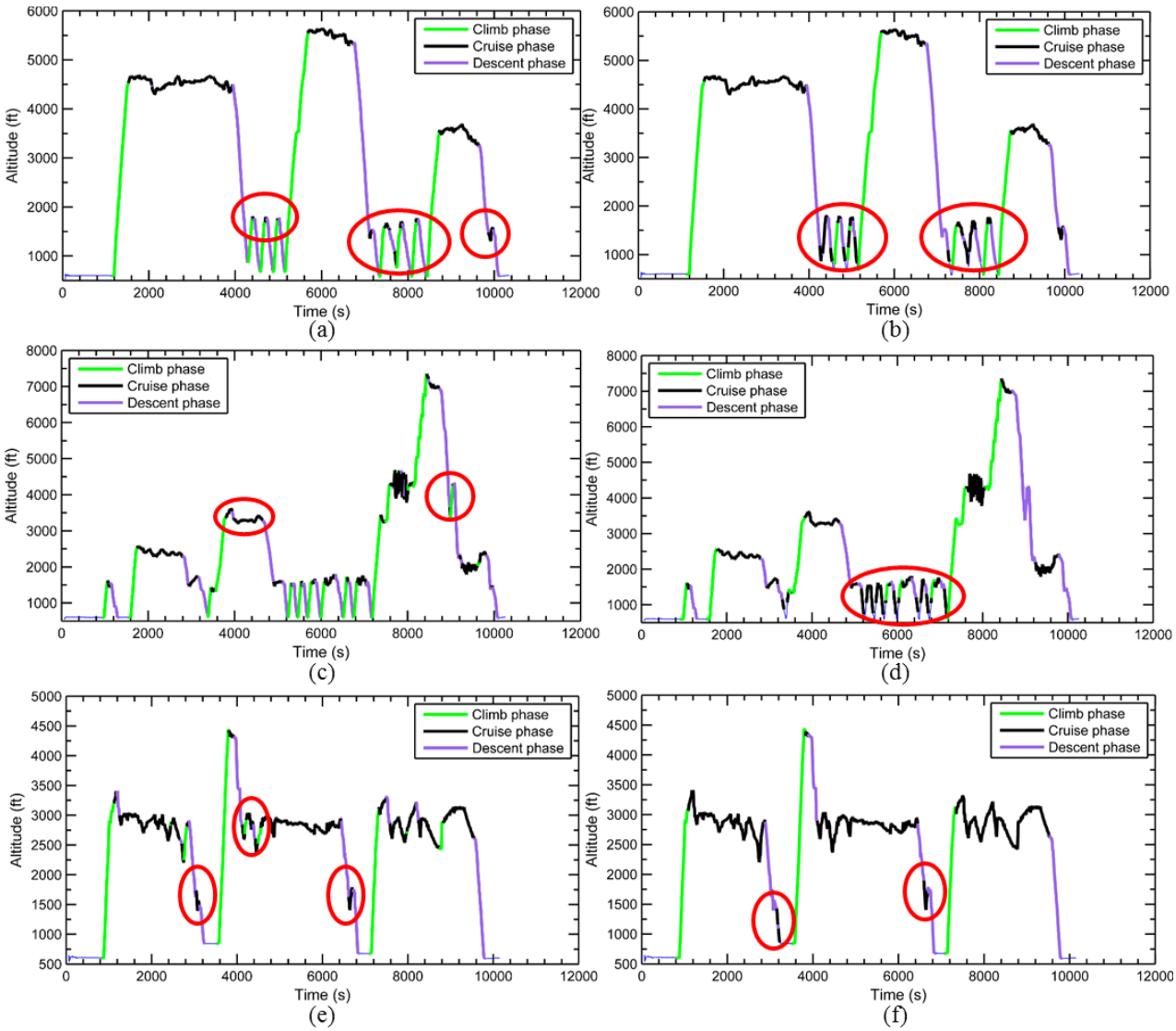

Figure 15: Moving average, rate of climb. *m* = 100 s for (a), (c), and (e), and *m* = 200 s for (b), (d), and (f).

Figure 15 shows the results of combining moving average smoothing and rate of climb for two values of *m* on three different flights. This combination of methods does not work as well as using the altitude difference method on our sample flights. In the first row, several points are misidentified as cruise, while in the third row, several cruise points are misidentified as climb/descent.

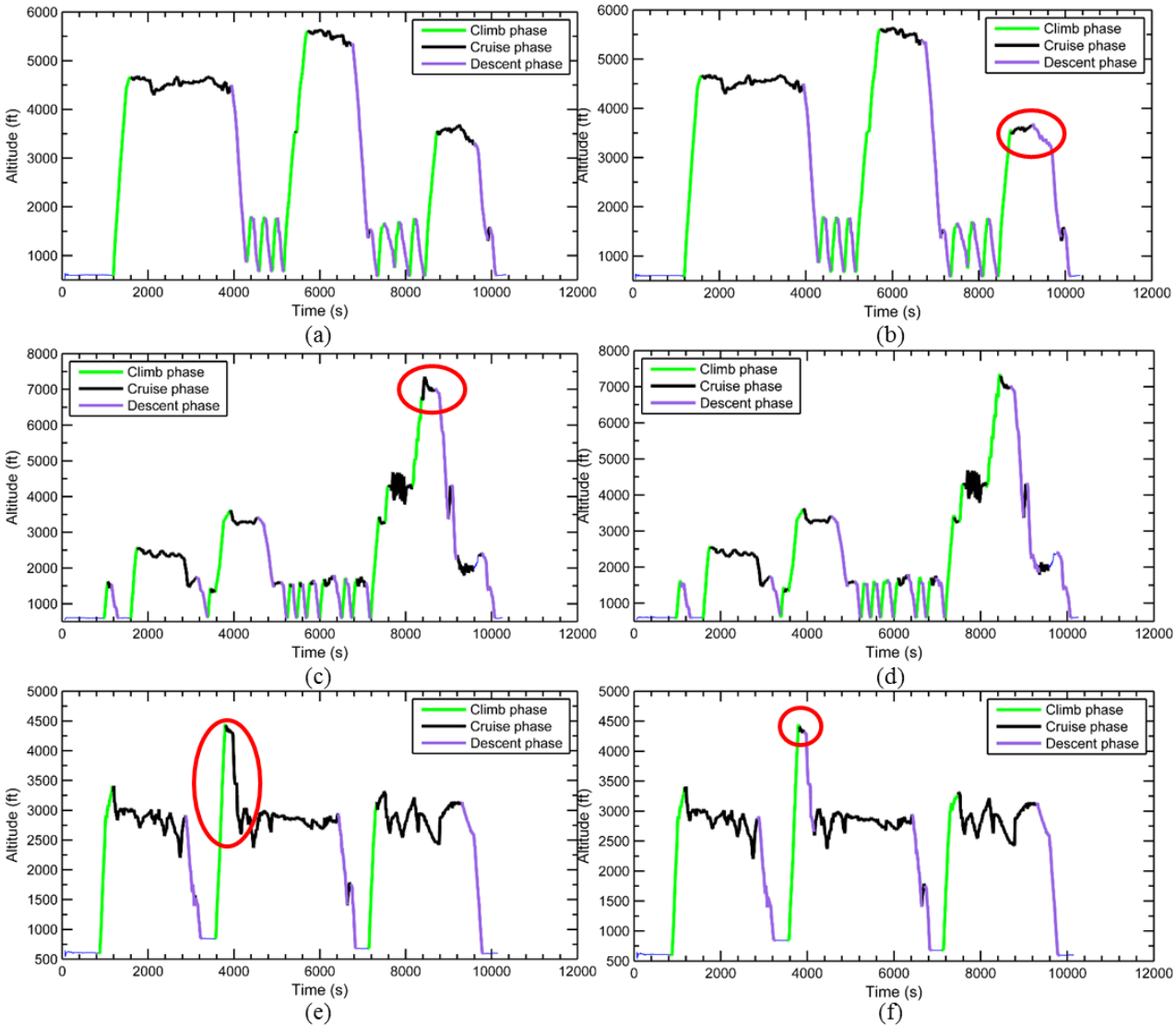

Figure 16: Local regression, altitude difference. p = 100 s for (a), (c), and (e), and p = 200 s for (b), (d), and (f).

Figure 16 shows the results of combining local regression smoothing and altitude difference for two values of p on three different flights. When the local regression window is smaller (left hand column), some climbs or descents are misidentified as cruise. This error is particularly noticeable on (e), where the descent starting at 3971 s is punctuated by several short level portions. The larger regression window (right column) combined with altitude difference provides the best results for our sample flights so far.

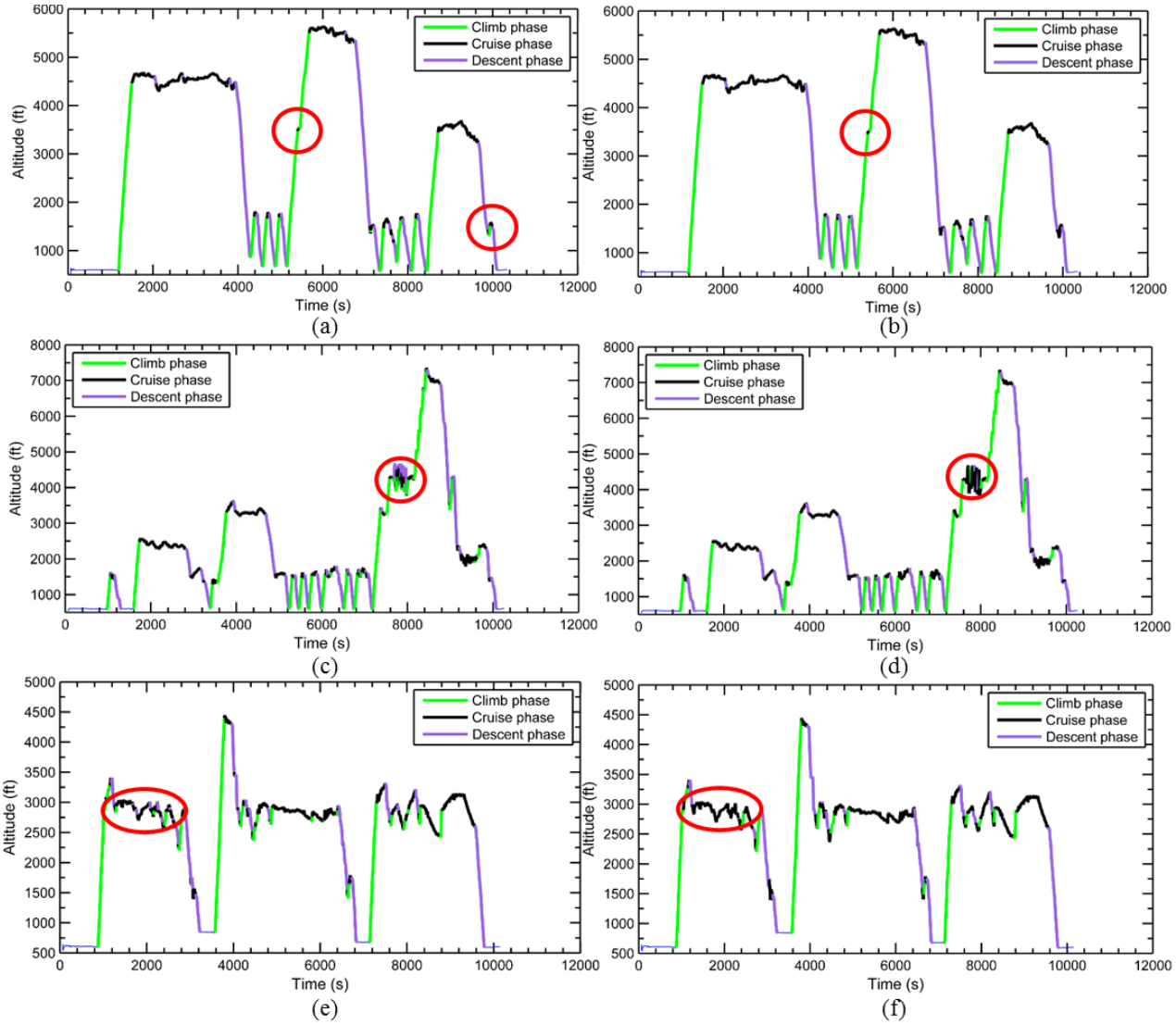

Figure 17: Local regression, rate of climb. p = 100 s for (a), (c), and (e), and p = 200 s for (b), (d), and (f).

Figure 17 shows the results of combining local regression smoothing and rate of climb for two values of p on three different flights. As with altitude difference, the smaller regression window results in some spurious cruise identifications (left hand column). The larger window results in some periods of rapid altitude change being identified as cruise (right hand column), especially for the second row (case (d)). Flight sample #9 (second row) contains the most complex variation of altitude of all samples available to us, and the circled segment was difficult to interpret. Either we consider that each variation has to be identified as a succession of climb and descent phases, or the overall segment is just cruise since the amplitude is constant and the duration of this segment is short. We chose the second option.

IV. Performance Comparison

In this section, we present the performance analysis of the two methods described in Section III. We first present the ideal solutions against which the methods will be evaluated and then assess the overall performance of the methods.

A. Metrics for performance evaluation

The algorithms' performance can be characterized using qualitative or quantitative methods, or a combination of both methods. For example, qualitative metrics include ease of use, and quantitative metrics include the algorithm's

speed of execution. In our initial evaluation, we focus on the proportion of misidentifications generated by each method on each of the 16 flights in our sample. Specifically, we calculate the error proportion as:

$$Error\ proportion = \frac{Incorrectly\ coded\ points}{Total\ points} \quad (1)$$

To determine when errors occurred, we hand-coded each of the sixteen flights. Figure 18 shows the result of hand-coding on samples #12, #9 and #1).

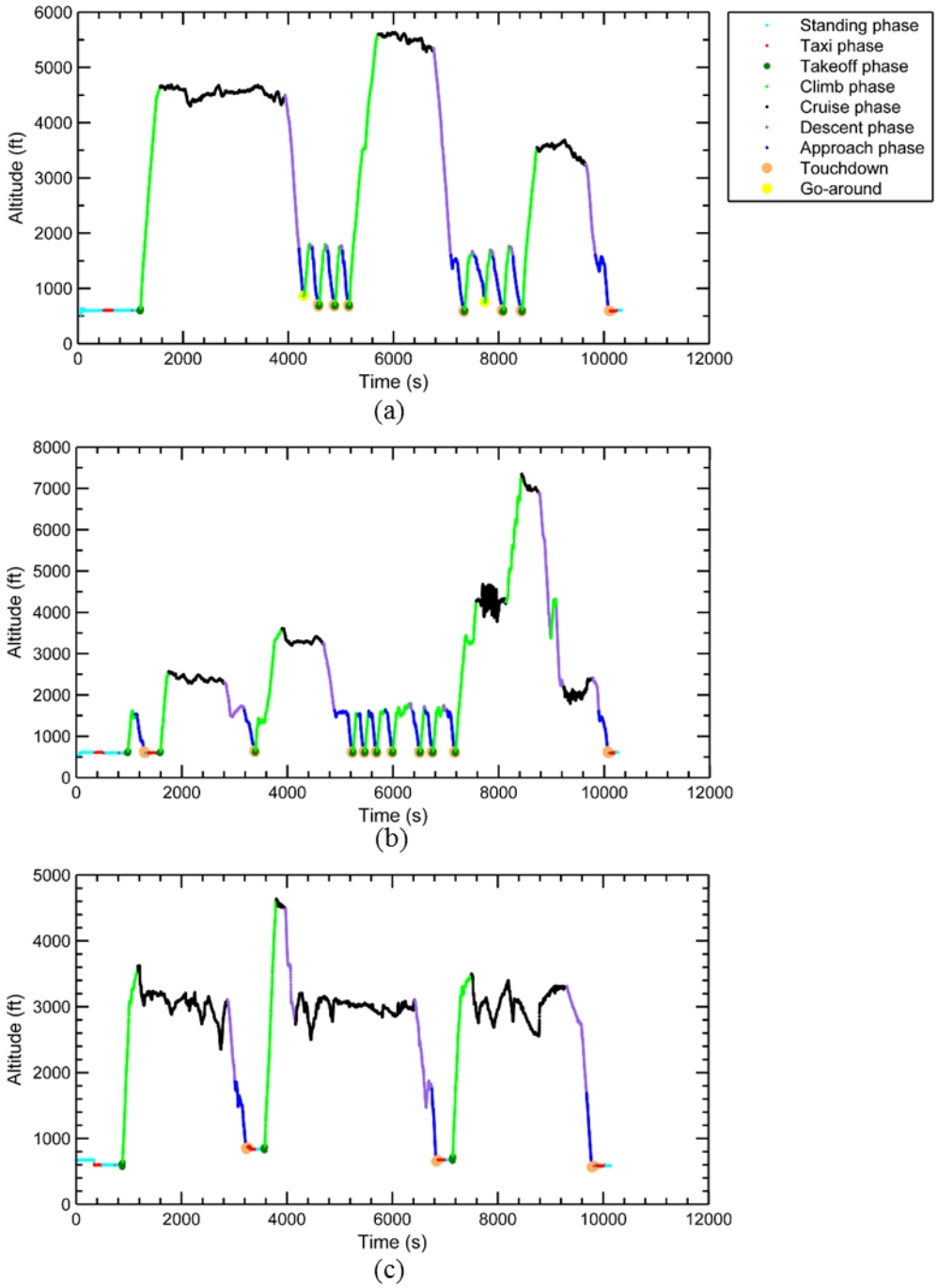

Figure 18: Three examples of "ideal" phases of flight detection for flight samples #12, #9 and #1 respectively.

Figure 18 shows that the interpretation of cruise (colored in black) depends on the type of flight. For example, in Figure 18 (c), the altitude varies significantly during cruise, while in (a) the cruise phases are relatively smooth. In addition, the altitude can vary significantly, even in small time windows. For example, in Figure 18 (a) at 4875 s and 8087 s, and in Figure 18 (b) at 5992 s, the rapid altitude variations represent patterns made around a particular airport or airfield. Those patterns can end by a Go-around as on Figure 18 (a), a full-stop, or just a touchdown before climbing and cruising again (touch-and-goes).

B. Discussion

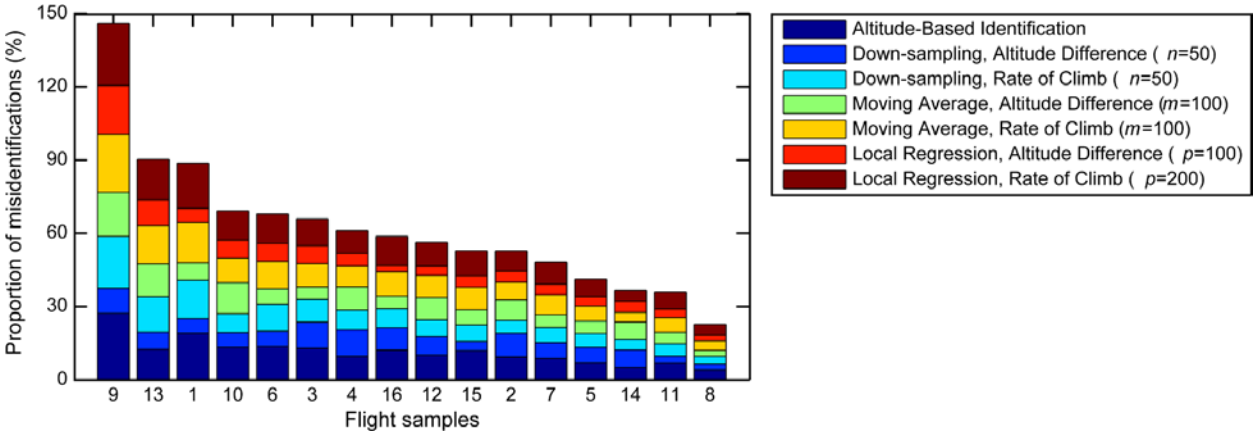

Figure 19: Flight samples sorted by decreasing proportions of misidentifications.

Figure 19 shows results from the performance measurement on our sixteen flight samples, using Method 1 and the six variations of Method 2. We tested each method with two different values for each characteristic parameter (n, m, and p) and selected the values that resulted in the fewest total errors across our sixteen samples. The samples are sorted from those with the most errors to those with the fewest errors. For each sample, the colors represent the different methods, and the percentage is the percentage of points that were incorrectly identified as defined by Equation (1). The figure shows that the algorithm performance depends on the characteristics of the flight sample. Sample #9 was the most difficult to assess automatically. This sample (see Figure 18 (b)) involves two very choppy cruise phases. In contrast, sample #8 had few errors, regardless of the method. This sample contains a more constant altitude for cruise segments and no altitude peaks as in Figure 18 (b).

As expected, Method 1 (Altitude-Based Identification) results in the most errors on the sixteen samples, as shown in Table 6. It results in the highest number of errors on eight of the samples. However, on flight samples #2, #4, and #14, the combination of Down-sampling and Altitude Difference performed the worst. All of these samples show constant cruise segments in terms of altitude but they also contain multiple patterns which cause a part of the misidentifications. For samples #5, #7, #8, #11, and #13, the highest proportion of misidentifications was caused by Local Regression followed by Rate of Climb, because these flights contain either a large variation of altitude during what should be considered as the cruise phase (especially sample #13) or long cruise segments. Therefore the weighted regression method is not appropriate for these sorts of flight. Overall, the lowest total errors are obtained using local regression and altitude difference. This method had the lowest number of errors on eight samples. The only samples where it performed worse were samples #3, #6, #9, #10, #11, #13, #14, and #15. Those are the samples that contain either the highest number of patterns, or the most unstable altitude during cruise phase.

Table 6: Average of proportion of misidentification for the seven methods, with parameters as shown.

Method	Average of proportion of misidentification
Altitude-Based Identification (Method 1)	11.47%
Local Regression, Rate of Climb (p = 200 s)	11.08%
Moving Average, Rate of Climb (m = 100 s)	9.94%
Down-sampling, Rate of Climb (n = 50)	8.64%
Moving Average, Altitude Difference (m = 100 s)	7.86%
Down-sampling, Altitude Difference (n = 50)	7.04%
Local Regression, Altitude Difference (p = 100 s)	6.11%

V. Conclusion and future work

We have presented initial work on automatically identifying phase of flight in General Aviation. Some phases of flight such as ground phases (Taxi, Standing) or Touchdown, Go-arounds, Takeoff and Approach are easily identified using simple relations based on parameters recorded by the on-board flight data recorder. However, Climb, Cruise and Descent are more difficult, due to the highly variable nature of GA flight. We developed two different approaches with several variants to identify these phases. We found that, while one variant was the best overall, different variants worked better or worse depending on the particular flight's characteristics, and, within a particular variant, the best parameter values also depend on the flight characteristics.

In future work, we will develop methods to select the best approach and the best associated parameter values. As part of GA-ASIAS, we will use the identification of phases of flight algorithm to detect safety events.

Acknowledgments

This research was partially funded by the US Department of Transportation/Federal Aviation Administration PEGASAS Center of Excellence under Award No 12-C-GA-PU AM8. The project was managed by Michael Vu. We thank Arjun Rao for his advice and insights.

The views expressed in this paper are those of the authors and do not necessarily reflect those of the FAA. The information in this research does not constitute FAA Flight Standards or FAA Aircraft Certification policy.

References

[1]GAMA, "General Aviation Statistical Databook & 2014 Industry Outlook", 2013.

[2]BTS, *Bureau of Transportation Statistics.* [Online] Available at: http://www.transtats.bts.gov/ [Accessed 27 April 2015].

[3]NTSB, "2013 Aviation Statistics". [Online] Available at: http://www.ntsb.gov/investigations/data/pages/aviation_stats.aspx [Accessed 27 April 2015].

[4]Harrison, E., Min, S., Jimenez, H. and Mavris, D. N., "Implementation and Validation of an Internal Combustion Engine and Propeller Model for General Aviation Aircraft Performance Studies", *Aviation 2015, AIAA*, Dallas, TX.

[5]Min, S., Harrison, E., Jimenez, H. and Mavris, D. N., "Development of Aerodynamic Modeling and Calibration Methods for General Aviation Aircraft Performance Analysis – a Survey and Comparison of Models", *Aviation 2015, AIAA*, Dallas, TX.

[6]Chati, Y. S. & Balakrishnan, H., "Aircraft Engine Performance Study Using Flight Data Recorder Archives". Los Angeles, California, 2013.

[7]SVETLANA, "Final publishable summary report", ACPO-GA-2010-265940, 2013.

[8]Paglione, M. & Oaks, R. O., "Determination of Horizontal and Vertical Phase of Flight in Recorded Air Traffic Data". *AIAA Guidance, Navigation, and Control Conference (GNC)*, Keystone, CO, American Institute of Aeronautics and Astronautics (AIAA), 2006.

[9]Paglione, M. & al., "Trajectory Prediction Accuracy Report: User Request Evaluation Tool (URET)/Center-TRACON Automation System (CTAS)", No. DOT/FAA/CT-TN99/10, Technical Center Atlantic City NJ: Federal Aviation Administration, 1999.

[10]Gong, C. & McNally, D., "A methodology for automated trajectory prediction analysis", *AIAA Guidance, Navigation, and Control Conference and Exhibit*, 2004.

[11]Nguyen, T. H. & Ward, D. T., "A neural-network based inference engine for a general aviation pilot advisor". *Reno, NV, 35th AIAA Aerospace Sciences Meeting and Exhibit*, 1997.

[12]Kelly, W. E. & Painter, J. H., "Flight segment identification as a basis for pilot advisory systems". *AIAA Journal of aircraft,* Issue 43.6, pp. 1628-1635, 2006.

[13]GPO, *Electronic Code of Federal Regulations, §61.109 Aeronautical experience.* [Online] Available at: http://www.ecfr.gov/ [Accessed 27 April 2015].

[14]NTSB, "Review of US Civil Aviation Accidents – Calendar Year 2011", 2014.

[15]Cirrus Design Corporation, *Airplane Information Manual for the Cirrus Design SR20, P/N 13999-002*, 1999.